125

Modeling of Contaminant Transport Resulting from Dissolution of Nonaqueous Phase Liquid Pools in Saturated Porous Media

CONSTANTINOS V. CHRYSIKOPOULOS[1],
EVANGELOS A. VOUDRIAS[2] and MARIOS M. FYRILLAS[3]
[1] *Department of Civil and Environmental Engineering, University of California, Irvine, CA 92717, U.S.A.*
[2] *School of Civil Engineering, Georgia Institute of Technology, Atlanta, GA 30332, U.S.A.*
[3] *Department of Mechanical and Aerospace Engineering, University of California, Irvine, CA 92717, U.S.A.*

Abstract. A mathematical model for transient contaminant transport resulting from the dissolution of a single component nonaqueous phase liquid (NAPL) pool in two-dimensional, saturated, homogeneous porous media was developed. An analytical solution was derived for a semi-infinite medium under local equilibrium conditions accounting for solvent decay. The solution was obtained by taking Laplace transforms to the equations with respect to time and Fourier transforms with respect to the longitudinal spatial coordinate. The analytical solution is given in terms of a single integral which is easily determined by numerical integration techniques. The model is applicable to both denser and lighter than water NAPL pools. The model successfully simulated responses of a 1,1,2-trichloroethane (TCA) pool at the bottom of a two-dimensional porous medium under controlled laboratory conditions.

Key words: NAPL pools, TCA dissolution, contaminant transport.

1. Notation

a, a_1 defined in (45a) and (45b), respectively

b ·   defined in (45c)

$\mathbf{b}$ vector of true model parameters $(n \times 1)$

$\hat{\mathbf{b}}$ vector of estimated model parameters $(n \times 1)$

c liquid phase solute concentration (solute mass/liquid volume), M/L^3

c_s aqueous saturation concentration (solubility), M/L^3

C dimensionless liquid phase solute concentration, equal to c/c_s

$\mathcal{D}$ molecular diffusion coefficient, L^2/t

$\mathcal{D}_e$ effective molecular diffusion coefficient, equal to $\mathcal{D}/\tau^*$, L^2/t

D_x longitudinal hydrodynamic dispersion coefficient, L^2/t

D_z hydrodynamic dispersion coefficient in the vertical direction, L^2/t

$\mathbf{e}$ random vector with zero mean $(m \times 1)$

$\text{erf}[x]$ error function, equal to $(2/\pi^{1/2}) \int_0^x e^{-z^2} dz$

$\mathbf{f}$ vector of fitting errors or residuals $(m \times 1)$

$\mathcal{F}$ Fourier operator

$\mathcal{F}^{-1}$ Fourier inverse operator

$\mathbf{g}$ vector of model simulated data $(m \times 1)$

k mass transfer coefficient, L/t

$\bar{k}$ average mass transfer coefficient, L/t

K_d partition or distribution coefficient (liquid volume/solids mass), L^3/M

ℓ pool length, L

ℓ_o distance between the pool and the origin of the specified Cartesian coordi-nate system, L

$\mathcal{L}$ Laplace operator

$\mathcal{L}^{-1}$ Laplace inverse operator

m number of observations

M Laplace/Fourier function defined in (38)

n number of model parameters

N Laplace/Fourier function defined in (39)

p defined in (46)

Pe_x Péclet number, equal to $U_x\ell/D_x$

Pe_z Péclet number, equal to $U_x\ell/D_z$

q defined in (47)

R retardation factor

s Laplace transform variable

S objective function

Sh local Sherwood number, equal to $k\ell/\mathcal{D}_e$

Sh_o overall Sherwood number, equal to $\bar{k}\ell/\mathcal{D}_e$

t time, t

T dimensionless time, equal to $U_x t/\ell$

u dummy integration variable

$\mathbf{u}$ vector of independent variables

U_x average interstitial velocity, L/t

x spatial coordinate in the longitudinal direction, L

X dimensionless longitudinal length, equal to $(x - \ell_o)/\ell$

$\mathbf{y}$ vector of observed data $(m \times 1)$

z spatial coordinate in the vertical direction, L

Z dimensionless vertical length, equal to z/ℓ

γ Fourier transform variable

ζ defined in (37)

η defined in (50)

θ porosity (liquid volume/aquifer volume), L^3/L^3

κ_1, κ_2 defined in (52a) and (52b), respectively

λ decay coefficient, t^{-1}

Λ dimensionless decay coefficient, equal to $\lambda\ell/U_x$

ρ bulk density of the solid matrix (solids mass/aquifer volume), M/L^3

τ dummy integration variable

τ^* tortuosity

2. Introduction

The contamination of natural subsurface systems by nonaqueous phase liquids (NAPLs), such as gasoline and organic solvents, has captured the attention of many environmental engineers and scientists. These liquids originate from leaking underground storage tanks, ruptured pipelines, surface spills, hazardous waste landfills, and disposal sites. As the number of contaminated sites increases so does the need for understanding the transport and fate of toxic NAPLs in the subsurface.

When a NAPL spill infiltrates the subsurface environment through the vadose zone, a portion of it may be trapped and immobilized within the unsaturated porous formation in the form of blobs or ganglia, which are no longer connected to the main body of the nonaqueous phase liquid (Hunt *et al.*, 1988a). Upon reaching the water table, NAPLs with densities heavier than that of water (sinkers, e.g., chlorinated solvents), given that the pressure head at the capillary fringe is sufficiently large, continue to migrate downward leaving behind trapped ganglia until they encounter an impermeable layer, where a flat source zone or pool with relatively small cross-section starts to form (Schwille, 1981, 1984; Anderson, 1988; Hunt *et al.*, 1988a; Mackay and Cherry, 1989). On the other hand, NAPLs with densities lower than that of water (floaters, e.g., petroleum products) as soon as they approach the saturated region spread laterally and float on the water table in the form of a pool (Schwille, 1981; Hunt *et al.*, 1988a). Sinker NAPL pools may further migrate along the formation contact only if the impermeable layer is inclined, whereas floater NAPL pools may move in the direction of decreasing hydraulic gradient.

As groundwater flows through trapped ganglia, a fraction of the NAPL dissolves in the aqueous phase and results in concentrations leaving the ganglia at or near saturation (Anderson *et al.*, 1992a). In contrast, pools have very low profiles and limited contact areas with respect to groundwater. If the same amount of NAPL is present as ganglia and as pool, ganglia dissolution is expected to proceed at a faster rate, because of the larger surface area available for interphase mass transfer (Schwille, 1988). Therefore, NAPL pools may lead to long-lasting sources

of groundwater contamination. If a floater NAPL pool is not stationary, NAPL dissolution will be influenced by the complicated flow characteristics of the two-phase system.

Although several theoretical and experimental studies associated with NAPL behavior in saturated as well as in unsaturated porous media have been reported (van der Waarden et al., 1971, 1977; Fried et al., 1979; Schwille, 1988; Pinder and Abriola, 1986; Hunt et al., 1988a, b; Miller et al., 1990; Mackay et al., 1991; Powers et al., 1991; Zalidis et al., 1991; Anderson et al., 1992a, b; Conrad et al., 1992; Johnson and Pankow, 1992, to mention a few), the literature on mathematical modeling, particularly on NAPL pool dissolution is rather limited. One of the few analytical models available has been derived by Hunt et al. (1988a). They presented an analytical solution to the two-dimensional steady-state advection-dispersion equation for NAPL pool dissolution in saturated semi-infinite homogeneous porous media. The model is suitable for nonreacting solutes and NAPL pools of approximately rectangular geometry.

This work is focused on the development of a mathematical model describing the transport of a decaying contaminant resulting from the dissolution of a single component NAPL pool formed at the bottom of a saturated, hydraulically homogeneous porous medium. Analytical procedures are employed to solve the two-dimensional advection-dispersion equation in conjunction with the appropriate initial and boundary conditions accounting for NAPL pool dissolution under uniform, steady interstitial fluid velocity. Although the mathematical solution is derived for denser than water NAPL pools, it can also be used for lighter than water NAPL pools by simply reversing the positive direction of the spatial coordinate z. The model is applied to an actual laboratory situation where 1,1,2-trichloroethane (TCA) is used to form a NAPL pool at the bottom of a two-dimensional porous medium.

3. Model Development

The transient contaminant transport from a dissolving NAPL pool denser than water as depicted schematically in Figure 1, assuming that the organic solvent is sorbing under local equilibrium conditions and undergoing a first-order decay, is governed by the following partial differential equation

$$R\frac{\partial c(t,\ x,\ z)}{\partial t} = D_x\frac{\partial^2 c(t,\ x,\ z)}{\partial x^2} + D_z\frac{\partial^2 c(t,\ x,\ z)}{\partial z^2} -$$

$$-U_x\frac{\partial c(t,\ x,\ z)}{\partial x} - \lambda Rc(t,\ x,\ z), \tag{1}$$

where $c(t,\ x,\ z)$ is the liquid phase solute concentration; U_x is the average interstitial fluid velocity; x, z are the spatial coordinates in the longitudinal and vertical directions, respectively; t is time; R is the dimensionless retardation factor,

introduced by Hashimoto *et al.* (1964), which for linear, reversible, instantaneous sorption is defined as

$$R = 1 + \frac{\rho}{\theta} K_d; \tag{2}$$

K_d is the partition or distribution coefficient and is expressed as the ratio of solute concentration on the adsorbent to solute aqueous concentration at equilibrium; ρ is the bulk density of the solid matrix; θ is porosity; D_x is the longitudinal hydrodynamic dispersion coefficient; D_z is the hydrodynamic dispersion coefficient in the vertical direction and λ is a first-order decay constant. It should be noted that the decay term λRc indicates that the total concentration (aqueous plus sorbed solute mass) disappear due to possible biological transformation. If the retardation factor is not included in the decay term the decay of the sorbed solute concentration is not accounted for. The governing two-dimensional partial differential equation considered is valid only for pools which are considerably wide in comparison to their length ℓ. Assuming that the thickness of the pool is insignificant relative to the thickness of the aquifer, and NAPL dissolution is described by the following mass transfer relationship, applicable at the NAPL-water interface

$$-\mathcal{D}_e \frac{\partial c(t,\, x,\, 0)}{\partial z} = k(t,\, x)[c_s - c(t,\, x,\, \infty)], \tag{3}$$

where $\mathcal{D}_e = \mathcal{D}/\tau^*$ is the effective molecular diffusion coefficient, $\mathcal{D}$ is the molecular diffusion coefficient, τ^* is the tortuosity [introduced by Carman (1937)], $k(t,\, x)$ is the mass transfer coefficient dependent on time and distance along the NAPL-water interface, c_s is the aqueous concentration at the interphase and for a pure organic liquid equals the liquid's aqueous saturation (solubility) concentration (Geller and Hunt, 1993), and $c(t,\, x,\, \infty) \simeq 0$ corresponds to the contaminant concentration outside the boundary layer, the appropriate initial and boundary conditions for this system are

$$c(0,\, x,\, z) = 0, \tag{4}$$

$$c(t,\, \pm\infty,\, z) = 0, \tag{5}$$

$$\mathcal{D}_e \frac{\partial c(t,\, x,\, 0)}{\partial z} = \begin{cases} 0 & x \leq \ell_o, \\ -k(t,\, x)c_s & \ell_o < x < \ell_o + \ell, \\ 0 & x \geq \ell_o + \ell, \end{cases} \tag{6}$$

$$c(t,\, x,\, \infty) = 0, \tag{7}$$

where ℓ_o is the distance between the pool and the origin of the specified Cartesian coordinate system, and ℓ is the pool length.
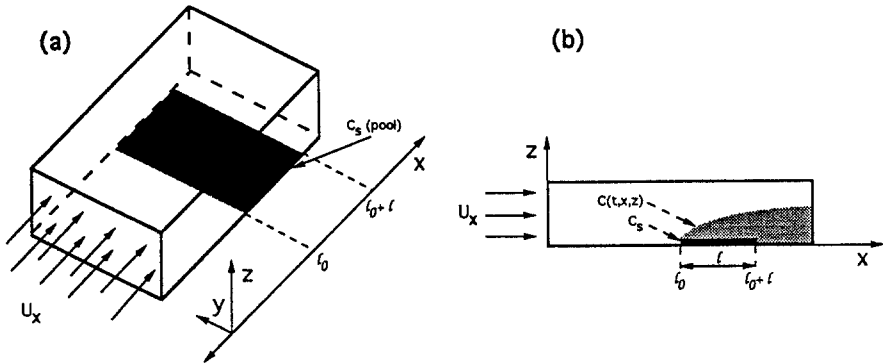
Fig. 1.   Schematic representation of (a) the conceptual physical model showing the unidirectional groundwater velocity, U_x, the location with respect to the origin of a Cartesian coordinate system of a denser than water NAPL pool with aqueous saturation concentration, C_s, and (b) an x–z cross-section showing the NAPL pool of length ℓ and the dissolved concentration $C(t, x, z)$.

It is generally more convenient to work with models written in dimensionless variables. By employing the following definitions

$$C = \frac{c}{c_s}, \tag{8}$$

$$X = \frac{x - \ell_o}{\ell}, \tag{9}$$

$$Z = \frac{z}{\ell}, \tag{10}$$

$$T = \frac{U_x t}{\ell}, \tag{11}$$

$$\text{Pe}_x = \frac{U_x \ell}{D_x}, \tag{12}$$

$$\text{Pe}_z = \frac{U_x \ell}{D_z}, \tag{13}$$

$$\Lambda = \frac{\lambda \ell}{U_x}, \tag{14}$$

$$\text{Sh}(T, X) = \frac{k(t, x)\ell}{\mathcal{D}_e}, \tag{15}$$

model equations (1) and (4)–(7) become

$$R\frac{\partial C(T, X, Z)}{\partial T} = \frac{1}{\text{Pe}_x}\frac{\partial^2 C(T, X, Z)}{\partial X^2} + \frac{1}{\text{Pe}_z}\frac{\partial^2 C(T, X, Z)}{\partial Z^2} -$$

$$-\frac{\partial C(T,\ X,\ Z)}{\partial X} - \Lambda R C(T,\ X,\ Z), \tag{16}$$

$$C(0,\ X,\ Z) = 0, \tag{17}$$

$$C(T,\ \pm\infty,\ Z) = 0, \tag{18}$$

$$\frac{\partial C(T,\ X,\ 0)}{\partial Z} = \begin{cases} 0, & X \le 0, \\ -\mathrm{Sh}(T,\ X), & 0 < X < 1, \\ 0, & X \ge 1, \end{cases} \tag{19}$$

$$C(T,\ X,\ \infty) = 0. \tag{20}$$

It should be noted that the dimensionless variable $\mathrm{Sh}(T,\ X)$ can be considered as a local Sherwood number.

Taking Laplace transforms with respect to the variable T of Equations (16), (19) and (20) yields

$$R[s\tilde{C}(s,\ X,\ Z) - C(0,\ X,\ Z)]$$

$$= \frac{1}{\mathrm{Pe}_x}\frac{\partial^2\tilde{C}(s,\ X,\ Z)}{\partial X^2} + \frac{1}{\mathrm{Pe}_z}\frac{\partial^2\tilde{C}(s,\ X,\ Z)}{\partial Z^2} -$$

$$- \frac{\partial\tilde{C}(s,\ X,\ Z)}{\partial X} - \Lambda R\tilde{C}(s,\ X,\ Z), \tag{21}$$

$$\frac{\partial\tilde{C}(s,\ X,\ 0)}{\partial Z} = \begin{cases} -\widetilde{\mathrm{Sh}}(s,\ X), & 0 < X < 1, \\ 0, & \text{otherwise}, \end{cases} \tag{22}$$

$$\tilde{C}(s,\ X,\ \infty) = 0, \tag{23}$$

where the following definitions were employed for the Laplace transformations (Spiegel, 1990)

$$\tilde{C}(s,\ X,\ Z) = \int_0^\infty C(T,\ X,\ Z)\,\mathrm{e}^{-sT}\,\mathrm{d}T, \tag{24}$$

$$\mathcal{L}\left\{\frac{\mathrm{d}C(T,\ X,\ Z)}{\mathrm{d}T}\right\} = s\tilde{C}(s,\ X,\ Z) - C(0,\ X,\ Z), \tag{25}$$

the tilde signifies Laplace transform, $\mathcal{L}$ is the Laplace operator and s is the transformed time variable. Employing (17) in (21) and then taking Fourier transforms with respect to space variable X of the resulting equation as well as of Equations

(22) and (23) leads to the following second-order ordinary differential equation and boundary conditions

$$Rs\hat{\tilde{C}}(s,\,\gamma,\,Z) = -\frac{\gamma}{\text{Pe}_x}\hat{\tilde{C}}(s,\,\gamma,\,Z) + \frac{1}{\text{Pe}_z}\frac{\text{d}^2\hat{\tilde{C}}(s,\,\gamma,\,Z)}{\text{d}Z^2} -$$

$$-i\gamma\hat{\tilde{C}}(s,\,\gamma,\,Z) - \Lambda R\hat{\tilde{C}}(s,\,\gamma,\,Z), \tag{26}$$

$$\frac{\text{d}\hat{\tilde{C}}(s,\,\gamma,\,0)}{\text{d}Z} = \frac{-1}{(2\pi)^{1/2}}\widehat{\widetilde{\text{Sh}}}(s,\,\gamma) * \Phi(\gamma)$$

$$= \frac{-1}{(2\pi)^{1/2}}\int_{-\infty}^{\infty}\widehat{\widetilde{\text{Sh}}}(s,\,\gamma-\omega)\Phi(\omega)\,\text{d}\omega, \tag{27}$$

$$\hat{\tilde{C}}(s,\,\gamma,\,\infty) = 0, \tag{28}$$

where

$$\Phi(\gamma) = \frac{1 - \text{e}^{-i\gamma}}{i\gamma(2\pi)^{1/2}}, \tag{29}$$

and the following definitions were employed for the Fourier transformations (Kreyszig, 1988)

$$\hat{\tilde{C}}(s,\,\gamma,\,Z) = \frac{1}{(2\pi)^{1/2}}\int_{-\infty}^{\infty}\tilde{C}(s,\,X,\,Z)\,\text{e}^{-i\gamma X}\,\text{d}X, \tag{30}$$

$$\mathcal{F}\left\{\frac{\text{d}\tilde{C}(s,\,X,\,Z)}{\text{d}X}\right\} = i\gamma\hat{\tilde{C}}(s,\,\gamma,\,Z), \tag{31}$$

$$\mathcal{F}\left\{\frac{\text{d}^2\tilde{C}(s,\,X,\,Z)}{\text{d}X^2}\right\} = -\gamma^2\hat{\tilde{C}}(s,\,\gamma,\,Z), \tag{32}$$

$$\mathcal{F}\left\{\begin{matrix} 1 & 0 < X < 1 \\ 0 & \text{otherwise} \end{matrix}\right\} = \frac{1 - \text{e}^{-i\gamma}}{i\gamma(2\pi)^{1/2}}, \tag{33}$$

$$\mathcal{F}\{f(X)g(X)\} = \frac{1}{(2\pi)^{1/2}}\hat{f}(\gamma) * \hat{g}(\gamma)$$

$$= \frac{1}{(2\pi)^{1/2}}\int_{-\infty}^{\infty}\hat{f}(\gamma-\omega)\hat{g}(\omega)\,\text{d}\omega, \tag{34}$$

the hat signifies Fourier transform, the asterisk indicates convolution, $\mathcal{F}$ is the Fourier operator, γ is the transformed spatial variable and $i = \sqrt{-1}$. Rearranging (26) yields

$$\frac{\mathrm{d}^2 \hat{\tilde{C}}(s, \gamma, Z)}{\mathrm{d}Z^2} - \mathrm{Pe}_z \left(\frac{\gamma^2}{\mathrm{Pe}_x} + i\gamma + Rs + R\Lambda \right) \hat{\tilde{C}}(s, \gamma, Z) = 0. \tag{35}$$

The solution to the preceding ordinary differential equation is

$$\hat{\tilde{C}}(s, \gamma, Z) = M(s, \gamma)\, \mathrm{e}^{\zeta Z} + N(s, \gamma)\, \mathrm{e}^{-\zeta Z}, \tag{36}$$

where

$$\zeta = (\mathrm{Pe}_z R)^{1/2} \left(\frac{\gamma^2}{\mathrm{Pe}_x R} + \frac{i\gamma}{R} + \Lambda + s \right)^{1/2}, \tag{37}$$

and $M(s, \gamma)$, $N(s, \gamma)$ are Laplace/Fourier functions which must be evaluated from boundary conditions. Applying boundary condition (27) in (36) yields that

$$M(s, \gamma) = 0. \tag{38}$$

In view of (27), (36) and (38) the unknown $N(s, \gamma)$ is evaluated to be

$$N(s, \gamma) = \frac{1}{\zeta (2\pi)^{1/2}} \int_{-\infty}^{\infty} \widehat{\widetilde{\mathrm{Sh}}}(s, \gamma - \omega) \Phi(\omega)\, \mathrm{d}\omega. \tag{39}$$

Substituting (38) and (39) into (36) leads to

$$\hat{\tilde{C}}(s, \gamma, Z) = \frac{\mathrm{e}^{-\zeta Z}}{\zeta (2\pi)^{1/2}} \int_{-\infty}^{\infty} \widehat{\widetilde{\mathrm{Sh}}}(s, \gamma - \omega) \Phi(\omega)\, \mathrm{d}\omega. \tag{40}$$

The inverse Laplace transformation of the preceding equation is

$$\hat{C}(T, \gamma, Z) = \frac{1}{\pi} \int_0^T \int_{-\infty}^{\infty} \left(\frac{1}{2\, \mathrm{Pe}_z\, R\tau} \right)^{1/2} \times$$

$$\times \exp \left[-\frac{\gamma^2 \tau}{\mathrm{Pe}_x R} - \frac{i\gamma \tau}{R} - \Lambda \tau - \frac{\mathrm{Pe}_z R Z^2}{4\tau} \right] \times$$

$$\times \widehat{\mathrm{Sh}}(T - \tau, \gamma - \omega) \Phi(\omega)\, \mathrm{d}\omega\, \mathrm{d}\tau, \tag{41}$$

where the following definitions and general properties of Laplace transforms were employed (Roberts and Kaufman, 1966; Spiegel, 1990)

$$\mathcal{L}^{-1}\{\tilde{f}(s - b)\} = f(T)\exp[bT], \tag{42}$$

$$\mathcal{L}^{-1}\left\{\frac{\exp[-as^{1/2}]}{a_1 s^{1/2}}\right\} = \frac{1}{a_1(\pi T)^{1/2}}\exp\left[\frac{-a^2}{4T}\right], \tag{43}$$

$$\mathcal{L}^{-1}\{\tilde{f}(s)\tilde{g}(s)\} = \int_0^T f(T-\tau)g(\tau)\,d\tau, \tag{44}$$

$$a = (\mathrm{Pe}_z RZ^2)^{1/2}, \qquad a_1 = (\mathrm{Pe}_z R)^{1/2}, \tag{45a,b}$$

$$b = -\left(\frac{\gamma^2}{\mathrm{Pe}_x R} + \frac{i\gamma}{R} + \Lambda\right), \tag{45c}$$

$\mathcal{L}^{-1}$ is the Laplace inverse operator, and τ is a dummy variable. In order to determine the inverse Fourier transformation of (41) with respect to γ, define the functions $p(X)$ and $q(X)$ as follows

$$p(X) = \mathcal{F}^{-1}\left\{\exp\left[-\frac{\gamma^2\tau}{\mathrm{Pe}_x R}\right]\exp\left[-\frac{i\gamma\tau}{R}\right]\right\}$$

$$= \left(\frac{\mathrm{Pe}_x R}{2\tau}\right)^{1/2}\exp\left[-\frac{\mathrm{Pe}_x R}{4\tau}\left(X - \frac{\tau}{R}\right)^2\right], \tag{46}$$

$$q(X) = \mathcal{F}^{-1}\left\{\frac{1}{(2\pi)^{1/2}}\int_{-\infty}^{\infty}\widehat{\mathrm{Sh}}(T-\tau, \gamma-\omega)\left[\frac{1-e^{-i\omega}}{i\omega(2\pi)^{1/2}}\right]d\omega\right\}$$

$$= \begin{cases} \mathrm{Sh}(T-\tau, X) & 0 < X < 1, \\ 0 & \text{otherwise,} \end{cases} \tag{47}$$

where the following shifting property is used

$$\mathcal{F}^{-1}\left\{\hat{f}(\gamma)\,e^{-i\gamma d}\right\} = f(X-d), \quad \text{with} \quad d = \frac{\tau}{R}, \tag{48}$$

$\mathcal{F}^{-1}$ is the Fourier inverse operator, and the inverse Fourier transforms were obtained from the tabulation of Kreyszig (1988). Direct application of the convolution theorem to $p(X)$ and $q(X)$ yields

$$\mathcal{F}^{-1}\{\hat{p}(\gamma)\hat{q}(\gamma)\} = \frac{1}{(2\pi)^{1/2}}\int_{-\infty}^{\infty}p(X-u)q(u)\,du$$

$$= \frac{1}{(2\pi)^{1/2}}\int_0^1\left(\frac{\mathrm{Pe}_x R}{2\tau}\right)^{1/2}\exp\left[-\frac{\mathrm{Pe}_x R}{4\tau}\left(X - u - \frac{\tau}{R}\right)^2\right] \times$$

$$\times \mathrm{Sh}(T-\tau, u)\,du, \tag{49}$$

where u is a dummy variable. Substituting the following expression

$$\eta = \left(X - u - \frac{\tau}{R} \right) \left(\frac{Pe_x R}{4\tau} \right)^{1/2},$$ (50)

into (49) yields

$$\mathcal{F}^{-1}\{\hat{p}(\gamma)\hat{q}(\gamma)\} = \frac{-1}{\pi^{1/2}} \int_{\kappa_1}^{\kappa_2} \exp[-\eta^2]\, Sh(T - \tau, u)\, d\eta,$$ (51)

where

$$\kappa_1 = \left(X - \frac{\tau}{R} \right) \left(\frac{Pe_x R}{4\tau} \right)^{1/2}, \quad \kappa_2 = \left(X - 1 - \frac{\tau}{R} \right) \left(\frac{Pe_x R}{4\tau} \right)^{1/2},$$ (52a,b)

$$u = X - \frac{\tau}{R} - \eta \left(\frac{4\tau}{Pe_x R} \right)^{1/2},$$ (53)

and the last formulation is derived from (50). In view of (41), (46), (47), and (51)–(53) the desired expression for $C(T, X, Z)$ is

$$C(T, X, Z) = -\frac{1}{\pi} \int_0^T \int_{\kappa_1}^{\kappa_2} \left(\frac{1}{Pe_z R\tau} \right)^{1/2} \exp\left[-\Lambda\tau - \frac{Pe_z R Z^2}{4\tau} \right] \times$$

$$\times \exp[-\eta^2]\, Sh(T - \tau, u)\, d\eta\, d\tau.$$ (54)

For the special case of an averaged mass transfer coefficient $k(t, x) = \bar{k}$, the local Sherwood number Sh can be replaced by the overall Sherwood number

$$Sh_o = \frac{\bar{k}\ell}{\mathcal{D}_e},$$ (55)

and (51) reduces to

$$\frac{-Sh_o}{\pi^{1/2}} \int_{\kappa_1}^{\kappa_2} \exp[-\eta^2]\, d\eta = \frac{Sh_o}{2}\{erf[\kappa_1] - erf[\kappa_2]\},$$ (56)

where the definition and fundamental properties of the error function have been applied (Gautschi, 1972). In view of (55) and (56) the solution for a constant mass transfer coefficient is

$$C(T, X, Z) = \frac{Sh_o}{2} \int_0^T \left(\frac{1}{\pi Pe_z R\tau} \right)^{1/2} \exp\left[-\Lambda\tau - \frac{Pe_z R Z^2}{4\tau} \right] \times$$

$$\times \left\{ erf\left[\left(X - \frac{\tau}{R} \right) \left(\frac{Pe_x R}{4\tau} \right)^{1/2} \right] - \right.$$

$$\left. - erf\left[\left(X - 1 - \frac{\tau}{R} \right) \left(\frac{Pe_x R}{4\tau} \right)^{1/2} \right] \right\} d\tau.$$ (57)
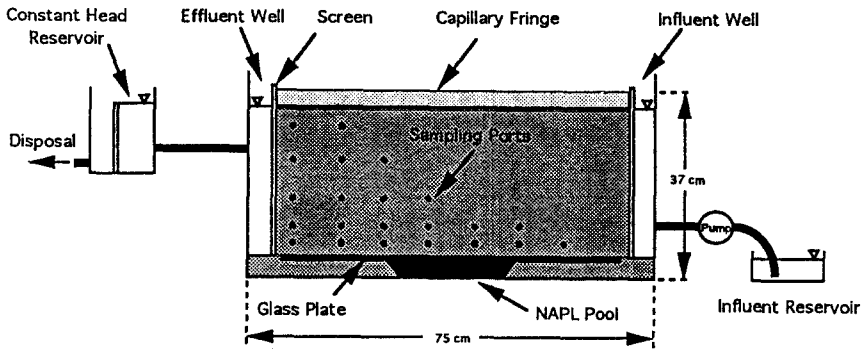
Fig. 2.   Schematic diagram showing the model aquifer and network of sampling ports.

4. Experimental Methods

4.1. DESIGN OF THE EXPERIMENTAL AQUIFER

A two-dimensional model aquifer (see Figure 2) was built to study the dissolution of a 1,1,2-trichloroethane (TCA) pool. The internal dimensions of the aquifer box were 75 cm in length, 37 cm in height, and 21 cm in width. The dimensions of the porous medium inside the aquifer were 65 cm in length, 34 cm in height, and 21 cm in width. In order to allow visual observation of the dissolution process, the walls of the model aquifer were constructed from 0.64 cm thick glass. The glass box was supported on an iron frame. In order to prevent leaking, all seams were caulked with silicone caulk. Two wells were constructed on the inlet and outlet of the glass tank to assist in the flow formation. Screens were installed inside the tank, 5 cm from each end, in order to prevent spilling of sand into the wells. Each screen consisted of 80 mesh stainless steel wire cloth, supported on a metal frame.

   A two-dimensional network of sampling ports was located in one of the side glass walls as shown in Figure 2. The location of the ports was decided on the basis of preliminary dissolution experiments conducted on a different tank. A series of 4 inch long 18 gauge stainless steel needles was inserted into the holes and pushed into the porous medium. Cleaning wires were kept inside the needles to prevent entrance of sand during the insertion step. The needles were caulked with silicone caulk. The Luer hubs of the needles were plugged with removable Teflon sampling valves.

4.2. FORMATION OF THE TCA POOL

A cooking pyrex pan with internal dimensions $28 \times 18 \times 4.5$ cm was used to confine the TCA pool at the bottom of the experimental aquifer. The empty aquifer box was filled with water to a depth of 5 cm and the empty pyrex pan was placed at the appropriate position at the bottom of the box. The pan was filled under water with aquarium gravel to a depth of 1.6 cm. At the top of the gravel, 20 to 30 mesh of

silica sand ($d_{50} = 690\,\mu m$) was added under water, until the pan was filled. The purpose of the gravel was to assist in the formation of a uniform pool, extending all the way to the bottom of the pan, which would not form if only sand was present in the pan. The pool formation technique was perfected after numerous trial and error experiments. A vertical glass pipet was inserted in the sand/gravel layer and was connected to a TCA reservoir with a pump. Then, the aquifer box was filled with sand by applying about 0.5 kg at a time with a beaker, under a water head of 5 cm maximum. The sand used in these experiments was silica sand. Two glass plates were placed horizontally at 5 cm from the bottom of the tank to provide a well-defined boundary at the bottom of the flow zone.

Tap water was used in all experiments and was stored in a large plastic container. The influent water contained 200 mg/L of sodium azide as a biocide to prevent biodegradation of TCA during the experiment. The flow of water into the aquifer was controlled with a variable speed pump. The water inlet was at the inlet well of the aquifer at 11.4 cm from the bottom of the well. The depth of the water table was controlled with an adjustable constant head reservoir connected with Teflon tubing to the outlet well of the model aquifer, with three connections at heights 4.5, 13.5, and 22.5 cm from the well bottom.

After the tank was flooded with water, the flow was stopped and the TCA pool was formed at the bottom of the aquifer by pumping TCA from the reservoir through the vertical pipet to the glass pan that was placed at the bottom of the tank. The TCA contained 1 g/L of water insoluble dye (Oil Red EGN dye) to assist in the visual observation of the pool during the tank excavation. The volume of TCA was calculated so that the TCA would fill the void space of the gravel layer and enter 2 cm inside the sand. Approximately 500 mL of TCA were used for the pool formation.

4.3. SAMPLE COLLECTION AND ANALYSIS

Interstitial water samples were collected from the syringe-needle sampling ports of the glass tank using Hamilton gas-tight syringes. After purging the needles with 0.3 mL of pore water, 1 mL of sample was withdrawn from each port and was immediately analyzed or stored in a headspace-free sample glass vial, sealed with teflon-lined septa. Storage time did not exceed 3 hours. The samples were analyzed by the 'purge-and-trap' procedure (EPA, 1982), using a gas chromatograph equipped with a flame ionization detector.

5. Nonlinear Regression Procedure

The two-dimensional transient NAPL dissolution model (Equation 57) is a nonlinear function of the dimensionless model parameters R, Pe_x, Pe_z and Λ. Thus, fitting the experimental data is a nonlinear estimation problem and iterative methods must be employed to compute the parameter estimates. There are several

approaches available for nonlinear parameter determination (Beck and Arnold, 1977). Here the nonlinear least squares regression method is adopted. In general, the objective of the nonlinear least squares method is to obtain estimates of the model parameters which minimize the residual sum of squares between simulated and observed data. The objective function may be written as

$$S(\hat{\mathbf{b}}) = [\mathbf{y} - \mathbf{g}(\mathbf{u}, \ \hat{\mathbf{b}})]^T [\mathbf{y} - \mathbf{g}(\mathbf{u}, \ \hat{\mathbf{b}})] = \mathbf{f}^T \mathbf{f}, \tag{58}$$

where $\mathbf{y} = \mathbf{g}(\mathbf{u}, \ \mathbf{b}) + \mathbf{e}$ is an $m \times 1$ observation vector, $\mathbf{g}$ is an $m \times 1$ vector of model simulated data, $\mathbf{u}$ is a vector of independent variables, $\mathbf{e}$ is an $m \times 1$ random vector with zero mean and known covariance matrix, $\mathbf{f}$ is $m \times 1$ vector of fitting errors or residuals.

Minimization of the objective function is not trivial, owing to the nonlinearities in $\mathbf{g}(\mathbf{u}, \ \mathbf{b})$. Several techniques have been developed for unconstrained nonlinear estimation. Simple iterative minimization algorithms, such as trial and error or exhaustive search, are seldom used due to inefficiency. However, there is a wide selection of nonlinear estimation methods which can be used for the least-squares estimation problem. The most frequently employed methods can be classified in two major categories, the modified Newton and Gauss-Newton linearization approaches. The first approach to the nonlinear estimation problem utilizes a Taylor series expansion to linearize the objective function, whereas the second approach for the nonlinear estimation problem is to expand the nonlinear model in a Taylor series around the initial parameter estimates. An advantageous modification of Gauss–Newton which is based on the work of Levenberg (1944) and Marquardt (1963), and eliminates potential numerical difficulties when a nonfull column rank Jacobian matrix is encountered. Here, the procedure known as the Levenberg–Marquardt method is employed.

6. Results and Discussion

6.1. MODEL SIMULATIONS

Consider a NAPL pool of length $\ell = 5$ m at the bottom of a homogeneous aquifer under steady, unidirectional flow. Furthermore, assume that the up-gradient or front end of the pool is located at a distance $\ell_o = 2$ m from the origin of a preselected Cartesian coordinate system, as shown in Figure 1. To predict dimensionless concentrations of the dissolved solvent in the vicinity of the pool, Equation (57) is employed. The integral over time is evaluated numerically by the extended Simpson's rule (Press et al., 1986). The range of model parameters used in the figures is chosen to encompass most of the commonly encountered groundwater conditions.

To illustrate the expected transient solvent distribution in the interstitial fluid of the hypothetical aquifer previously described, contours of dimensionless concentrations for a conservative solvent (nonsorbing, nonreacting) in the vertical
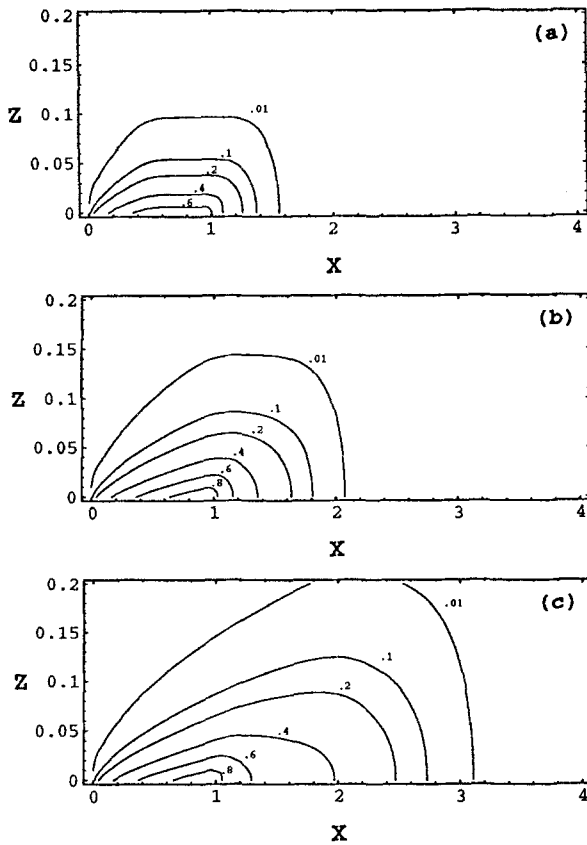
Fig. 3.   Lines of equal dimensionless concentration plotted in the XZ plane for (a) $T = 0.5$, (b) $T = 1$ and (c) $T = 2$ ($R = 1$, $Pe_x = 125$, $Pe_z = 500$, $Sh_o = 20$, $\Lambda = 0$).

to the pool plane for three different points in time are presented in Figure 3. It should be noted that for the dimensionless coordinate system employed here the nonaqueous phase liquid pool is located at $0 \le X \le 1$. Careful inspection of these contours reveals that predicted dissolved dimensionless concentrations at a given vertical height increase with distance from the up-gradient end of the pool; at some distance beyond the down-gradient end of the pool a peak concentration is reached and further downstream the longitudinal and vertical dispersion cause the concentrations to decline with distance. Figure 4 illustrates the effect of normalized vertical distance from the pool on dissolved dimensionless concentrations. As the distance from the pool gets larger, concentration levels decrease and the position of the point of maximum concentration shifts away from the pool.

The effect of Pe_x on dimensionless dissolved concentration profiles at a normalized vertical height of $Z = 0.02$ and $T = 1$ is shown in Figure 5. The higher the value of Pe_x the higher the dimensionless peak concentration and the smaller the spreading of the solute. This result was expected because an increase in Pe_x
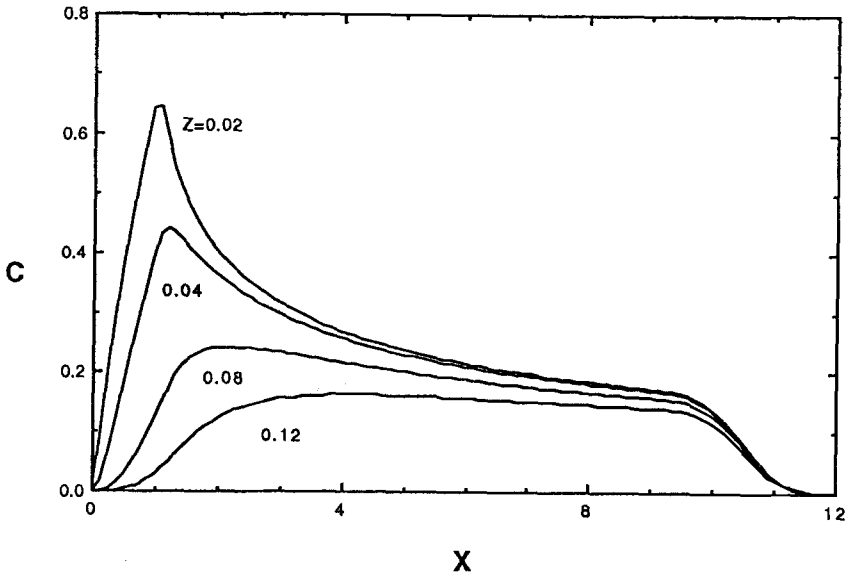
Fig. 4. Variation of dimensionless concentration with normalized distance in the direction of flow for different normalized distances in the vertical direction ($R = 1$, $Pe_x = 125$, $Pe_z = 500$, $Sh_o = 20$, $\Lambda = 0$, $T = 10$).

implies a decrease in the longitudinal dispersion coefficient. Similarly, in Figure 6 we have presented dimensionless concentration profiles for three values of Pe_z. It is evident from this illustration that increasing Pe_z or equivalently decreasing the hydrodynamic dispersion coefficient in the vertical direction, the dimensionless concentration decreases. By comparing Figures 5 and 6 it is clear that the dissolved concentration is sensitive to the value of Pe_z.

The effect of retardation factor on dissolved dimensionless concentration profiles for two values of Λ is illustrated in Figure 7. The solid lines correspond to $\Lambda = 0$ and the dotted lines to $\Lambda = 0.15$. At early time ($T = 0.5$), dissolved dimensionless concentrations decrease with increasing retardation factor; however, for the case of $\Lambda \neq 0$ the concentrations are slightly lower due to solute decay (see Figure 7a). At large time ($T = 20$), the magnitude of the retardation factor, as shown in Figure 7b, has no longer an effect on dimensionless concentration distributions within the homogeneous aquifer for the case where $\Lambda = 0$, but for $\Lambda \neq 0$ the dissolved concentrations are dependent on R. Thus, for a decaying solvent the dissolved concentration distributions are dependent on the retardation factor at all time.

6.2. MODEL CALIBRATION

Due to experimental difficulties, TCA breakthrough data were observed only at sampling ports P31, located 8.1 cm from the front end of the pool at a vertical
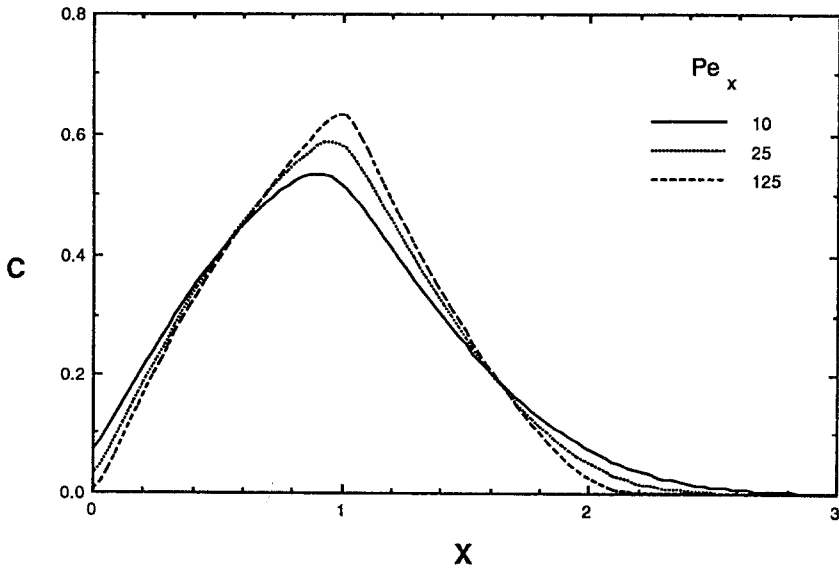
Fig. 5. Distribution of dimensionless concentration vs normalized distance in the direction of flow for $Pe_x = 10$, 25, 125 ($R = 1$, $Pe_z = 500$, $Z = 0.02$, $Sh_o = 20$, $\Lambda = 0$, $T = 1$).
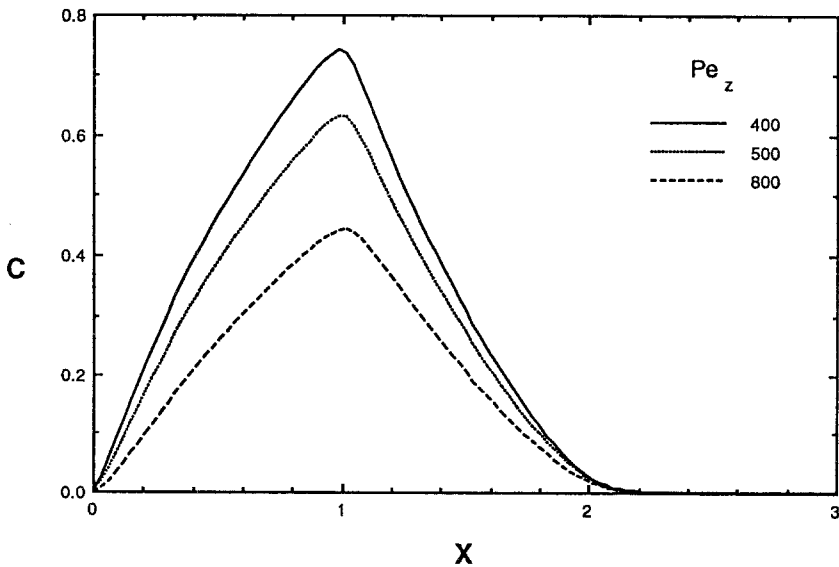

Fig. 6. Distribution of dimensionless concentration vs normalized distance in the direction of flow for $Pe_z = 400$, 500, 800 ($R = 1$, $Pe_x = 125$, $Z = 0.02$, $Sh_o = 20$, $\Lambda = 0$, $T = 1$).

distance of 2.75 cm from the pool surface, or in dimensionless notation $(X, Z) = (0.289, 0.098)$, P41 $(0.643, 0.088)$ and P51 $(1.004, 0.088)$. The pool length was $\ell = 0.28\,\mathrm{m}$, and the solubility of TCA at 20°C is 4,500 mg/L (Verschueren, 1983). Only three model parameters are unknown because a retardation factor of $R = 1.1$
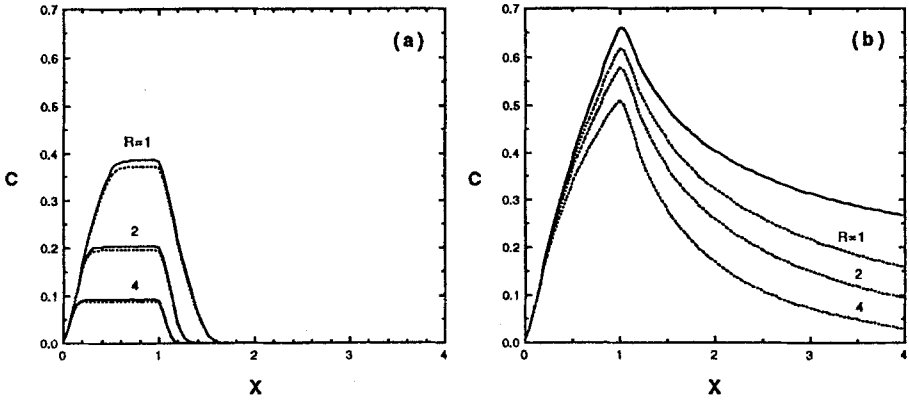
Fig. 7. Variation of dimensionless concentration with normalized distance in the direction of flow for different retardation factors with $\Lambda = 0$ (solid lines) and $\Lambda = 0.15$ (dotted lines) at (a) $T = 0.5$, and (b) $T = 20$ (Pe$_x = 125$, Pe$_z = 500$, $Z = 0.02$, Sh$_o = 20$, $\Lambda = 0$).

was obtained from batch sorption experiments with TCA and aquifer sand, and Λ is zero because TCA is practically a nondecaying organic [its environmental half-life for abiotic decomposition is 170 years (Vogen et al., 1987)]. The best estimates of the three unknown parameters were obtained by the estimation methodology previously described as follows: Pe$_x = 85.6$, Pe$_z = 213.4$, and Sh$_o = 13.4$. Given that the average interstitial velocity was measured in the experiment as $U_x = 0.00349$ m/h, the molecular diffusion coefficient for TCA in bulk water was estimated by the Wilke–Chang equation as $\mathcal{D} = 2.92 \times 10^{-6}$ m^2/h (Lyman et al., 1982), and for sands $\tau^* = 1.43$ (de Marsily, 1981, p. 233), in view of (12), (13) and (55) we can evaluate $D_x = 1.14 \times 10^{-5}$ m^2/h, $D_z = 4.59 \times 10^{-6}$ m^2/h, and $\bar{k} = 9.78 \times 10^{-5}$ m/h.

The actual TCA data observed at sampling ports P31, P41 and P51 together with the model simulated profiles are shown in Figure 8. Good agreement between the experimental data and simulated concentration history is shown for all cases. Clearly, the observed data incorporate some experimental error, caused mainly by slight fluctuations in U_x. Such variations in the observed data cannot be simulated. Due to the relatively small size of the experimental data set available, only model calibration was performed and a verification of the analytical solution based on 'blind' prediction was not carried out.

7. Summary and Concluding Remarks

An analytical solution to a two-dimensional transient model describing contaminant transport from NAPL pool dissolution has been developed, and some of the features of the solution have been illustrated. The model assumes that the porous medium is homogeneous, the interstitial groundwater velocity steady and the organic solute may undergo linear reversible, instantaneous sorption. Although
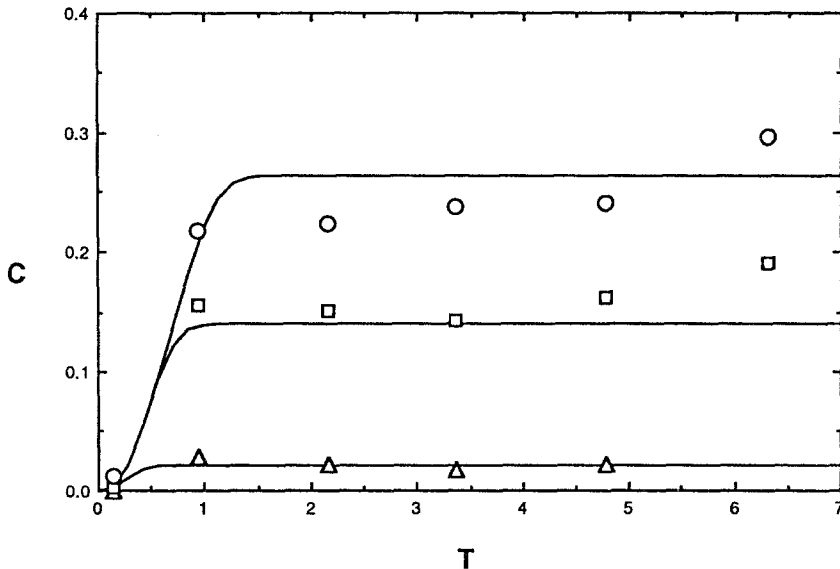
Fig. 8.   TCA concentration experimental data observed at sampling ports P31 (triangles), P41 (squares), P51 (circles) and simulated concentration history (solid curves).

the model presented has many advantages due to its analytical nature, some of the limitations inherent to the model are its inability: (a) to allow for spatially variable velocity field; (b) to account for the more realistic case of spatially variable sorption or geochemical characteristics; and (c) to allow for multicomponent NAPL dissolution.

TCA concentration profiles, obtained from controlled laboratory experiments, were used to calibrate the model. Parameter estimates for Pe_x, Pe_z and Sh_o were determined by nonlinear least squares regression. Good agreement was shown between the experimental data and the simulated concentration profiles.

Acknowledgements

References

Anderson, M. R., 1988, The dissolution and transport of dense non-aqueous phase liquids in saturated porous media, PhD dissertation, Oregon Graduate Institute, Beaverton, Oregon.
Anderson, M. R., Johnson, R. L., and Pankow, J. F., 1992a, Dissolution of dense chlorinated solvents into groundwater, 1, Dissolution from a well-defined residual source, *Ground Water* **30**(2), 250–256.

Anderson, M. R., Johnson, R. L., and Pankow, J. F., 1992b, Dissolution of dense chlorinated solvents into groundwater, 3, Modeling contaminant plumes from fingers and pools of solvent, *Environ. Sci. Technol.* **26**(5), 901–908.

Beck, J. V. and Arnold, K. J., 1977, *Parameter Estimation in Engineering and Science*, Wiley, New York.

Carman, P. C., 1937, Fluid flow through granular beds, *Trans. Inst. Chem. Eng. London* **15**, 150–156.

Conrad, S. H., Wilson, J. L., Mason, W. R., and Peplinski, W. J., 1992, Visualization of residual organic liquid trapped in aquifers, *Water Resour. Res.* **28**(2), 467–478.

de Marsily, G., 1981, *Quantitative Hydrogeology, Groundwater Hydrology for Engineers*, Academic Press, San Diego, California.

EPA, 1982, Test methods for organic chemical analysis of municipal and industrial wastewater, EPA-600/4-82-057.

Fried, J. J., Muntzer, P., and Zilliox, L., 1979, Ground-water pollution by transfer of oil hydrocarbons, *Ground Water* **17**(6), 586–594.

Gautschi, W., 1972, Error function and fresnel integrals, in M. Abramowitz and I. A. Stegun (eds) *Handbook of Mathematical Functions*, Wiley-Interscience, pp. 209–329.

Geller, J. T. and Hunt, J. R., 1993, Mass transfer from nonaqueous phase organic liquids in water-saturated porous media, *Water Resour. Res.* **29**(4), 833–845.

Hashimoto, I., Deshpande, K. B., and Thomas, H. C., 1964, Péclet numbers and retardation factors for ion exchange columns, *Ind. Eng. Chem. Fundam.* **3**(3), 213–218.

Hunt, J. R., Sitar, N., and Udell, K. S., 1988a, Nonaqueous phase liquid transport and cleanup, 1, Analysis of mechanisms, *Water Resour. Res.* **24**(8), 1247–1258.

Hunt, J. R., Sitar, N., and Udell, K. S., 1988b, Nonaqueous phase liquid transport and cleanup, 2, Experimental studies, *Water Resour. Res.* **24**(8), 1259–1269.

Johnson, R. L. and Pankow, J. F., 1992, Dissolution of dense chlorinated solvents into groundwater, 2, Source functions for pools of solvent, *Environ. Sci. Technol.* **26**(5), 896–901.

Kreyszig, E., 1988, *Advanced Engineering Mathematics*, 6th edn, Wiley, New York.

Levenberg, K., 1944, A method for the solution of certain nonlinear problems in least squares, *Quart. Appl. Math.* **2**, 164–168.

Lyman, W. J., Reehl, W. F., and Rosenblatt, D. H., 1982, *Handbook of Chemical Property Estimation Methods*, McGraw-Hill, New York.

Mabey, W. R., Smith, J. H., Podoll, R. T., Johnson, H. L., Mill, T., Chou, T.-W., Gates, J., Partridge, I. W., Jaber, H., and Vendenberg, D., 1982, Aquatic fate process data for organic priority pollutants, Tech. Report 440/4-81-014, U.S. Environmental Protection Agency, Washington, D.C.

Mackay, D., Shiu, W. Y., Maijanen, A., and Feenstra, S., 1991, Dissolution of non-aqueous phase liquids in groundwater, *J. Contam. Hydrol.* **8**, 23–42.

Mackay, D. M. and Cherry, J. A., 1989, Groundwater contamination: Pump-and-treat remediation, *Environ. Sci. Technol.* **23**(6), 630–636.

Marquardt, D. W., 1963, An algorithm for least-squares estimation of nonlinear parameters, *SIAM J. Appl. Math.* **11**(2), 431–441.

Miller, C. T., Poirier-McNeill, M. M., and Mayer, A. S., 1990, Dissolution of trapped nonaqueous phase liquids: Mass transfer characteristics, *Water Resour. Res.* **26**(11), 2783–2796.

Pinder, G. F. and Abriola, L. M., 1986, On the simulation of nonaqueous phase organic compounds in the subsurface, *Water Resour. Res.* **22**(9), 109s–119s.

Powers, S. E., Loureiro, C. O., Abriola, L. M., and Weber, Jr., W. J., 1991, Theoretical study of the significance of nonequilibrium dissolution of nonaqueous phase liquids in subsurface systems, *Water Resour. Res* **27**(4), 463–477.

Press, W. H., Flannery, B. P., Teukolsky, S. A., and Vetterling, W. T., 1986, *Numerical Recipes: The Art of Scientific Computing*, Cambridge University Press, New York.

Roberts, G. E. and Kaufman, H., 1966, *Table of Laplace Transforms*, W. B. Saunders, Philadelphia, PA.

Schwille, F., 1981, Groundwater pollution in porous media by fluids immiscible with water, in W. van Diujvenbooden, P. Glasberger, and H. H. Lelyveld (eds), *Quality of Groundwater, Studies in Environmental Science*, vol. 17, Elsevier Science, New York, pp. 451–463.

Schwille, F., 1984, Migration of organic fluids immiscible with water, in *Pollutants in Porous Media*, Ecol. Stud., vol. 47, Springler-Verlag, New York, pp. 27–48.

Schwille, F., 1988, *Dense Chlorinated Solvents in Porous and Fractured Media*, Translated by J. F. Pankow, Lewis Publishers, Chelsea, Michigan.

Spiegel, M. R., 1990, *Laplace Transforms*, McGraw-Hill, New York.

van der Waarden, M., Bridié, A. L. A. M., and Groenewoud, W. M., 1971, Transport of mineral oil components to groundwater, 1, Model experiments on the transfer of hydrocarbons from a residual oil zone to trickling water, *Water Res.* **5**, 213–226.

van der Waarden, M., Groenewoud, W. M., and Bridié, A. L. A. M., 1977, Transport of mineral oil components to groundwater, 2, Influence of lime, clay and organic soil components on the rate of transport, *Water Res.* **11**, 359–365.

Verschueren, K., 1983, *Handbook of Environmental Data on Organic Chemicals*, 2nd edn, Van Nostrand Reinhold, New York.

Vogel, T. M., Criddle, C. S., and McCarty, P. L., 1987, Transformations of halogenated aliphatic compounds, *Environ. Sci. Technol.* **21**(8), 722–736.

Zalidis, G. C., Annable, M. D., Wallace, R. B., Hayden, N. J., and Voice, T. C., 1991, A laboratory method for studying the aqueous phase transport of dissolved constituents from residually held NAPL in unsaturated soil columns, *J. Contam. Hydrol.* **8**, 143–156.